Journal of
Mechanics of
Materials and Structures

INDENTATION ANALYSIS OF FRACTIONAL VISCOELASTIC SOLIDS

Rouzbeh Shahsavari and Franz-Josef Ulm

Volume 4, Nº 3 March 2009

mathematical sciences publishers

JOURNAL OF MECHANICS OF MATERIALS AND STRUCTURES
Vol. 4, No. 3, 2009

INDENTATION ANALYSIS OF FRACTIONAL VISCOELASTIC SOLIDS

ROUZBEH SHAHSAVARI AND FRANZ-JOSEF ULM

The constitutive differential equations governing the time-dependent indentation response for axisymetric indenters into a fractional viscoelastic half-space are derived, together with indentation creep and relaxation functions suitable for the backanalysis of fractional viscoelastic properties from indentation data. These novel fractional viscoelastic indentation relations include, as a subset, classical integer-type viscoelastic models such as the Maxwell model or Zener model. Using the correspondence principle of viscoelasticty, it is found that the differential order of the governing equations of the indentation response is higher than the one governing the material level. This difference in differential order between the material scale and indentation scale is more pronounced for the viscoelastic shear response than for the viscoelastic bulk response, which translates, into fractional derivatives, the well-known fact that an indentation test is rather a shear test than a hydrostatic test. By way of example, an original method for the inverse analysis of fractional viscoelastic properties is proposed and applied to experimental indentation creep data of polystyrene. The method is based on fitting the time-dependent indentation data (in the Laplace domain) to the fractional viscoelastic model response. Applied to polysterene, it is shown that the particular time-dependent response of this material is best captured by a bulk-and-deviator fractional viscoelastic model of the Zener type.

1. Introduction

The aim of indentation analysis is to link indentation data, typically an indentation force versus indentation depth curve, F-h, to meaningful mechanical properties of the indented material. It is common practice to condense the indentation data into two quantities, the hardness H and the indentation modulus M, which are related to measured indentation data, namely the maximum indentation force $F_{\max}$, the initial slope (or indentation stiffness) S of the unloading curve, and the projected contact area A_c by

$$H \stackrel{\text{def}}{=} \frac{F_{\max}}{A_c}, \qquad S = \frac{dF}{dh}|_{h=h_{\max}} \stackrel{\text{def}}{=} \frac{2}{\sqrt{\pi}} M \sqrt{A_c}. \tag{1}$$

Traditionally, for metals, the hardness H was early on recognized to relate to strength properties of the indented material [Brinell 1901; Tabor 1951], and recent developments in indentation analysis have extended those approaches to account for strain hardening [Cheng and Cheng 2004], cohesive-frictional strength behavior [Ganneau et al. 2006], and the effect of porosity on the strength behavior [Cariou et al. 2008]. The investigation of the link between the unloading slope S and the elasticity properties of the indented material is more recent, requiring depth sensing indentation techniques that provide a continuous

Keywords: fractional viscoelasticity, indentation analysis, creep, relaxation, correspondence principle, polysterene.
This work was supported by Schoettler Fellowship Program at MIT, and Schlumberger–Doll Research, Cambridge, MA. The experimental data on Polystyrene was provided by Dr. Catherine Tweedie and Prof. Krystyn J. Van Vliet, of MIT's Department of Material Science and Engineering.

Indenter shape	n	B	ϕ	F-h relation
Cone	1	$\cot\theta$	$\frac{2\tan\theta}{\pi}$	$F=\frac{2M\tan\theta}{\pi}h^2$
Sphere	2	$1/2R$	$\frac{4\sqrt{R}}{3}$	$F=\frac{4M\sqrt{R}}{3}h^{1.5}$
Flat punch	$\to\infty$	$1/a^n$	$2a$	$F=2Mah$

Table 1. F-h equations for different indenter shapes. θ is the half-cone angle, R and a are the sphere radius and the flat cylinder punch, respectively.

record of the F-h curve during loading and unloading in an indentation test [Tabor 1951; Doerner and Nix 1986; Oliver and Pharr 1992; Bulychev 1999]. Relation $(1)_2$ is an exact relation for linear elastic materials. For non-elastic materials, $(1)_2$ becomes an approximate relation and S may be affected by the residual stress field and by adhesion of materials [Borodich and Galanov 2008]. Application of the depth sensing indentation techniques in indentation analysis confirmed the link provided by classical linear elastic contact mechanics solutions [Hertz 1882; Boussinesq 1885; Love 1939; Galin 1961; Sneddon 1965; Borodich and Keer 2004] for a rigid indenter of axysmmetric shape that can be described by a monomial function of the form $z=Br^n$:

$$F=\phi Mh^{1+1/n}, \tag{2}$$

where r and z are, respectively, the first and the third cylindrical coordinates of the surface of the tip, ϕ (of dimension $[\phi]=L^{1-1/n}$), condenses the indenter specific geometry parameters,

$$\phi=\frac{2}{(\sqrt{\pi}B)^{1/n}}\frac{n}{n+1}\left[\frac{\Gamma(n/2+1/2)}{\Gamma(n/2+1)}\right]^{1/n}, \tag{3}$$

B is the shape function of the indenter at unit radius, $n\geq 0$ is the degree of the homogeneous function, $\Gamma(x)$ is the Euler Gamma function, $\Gamma(x)=\int_0^\infty t^{x-1}\exp(-t)dt$. Table 1 develops expression (2) for some common indenter shapes. Finally, M is the indentation modulus. The indentation modulus M provides a snapshot of the elasticity of the indented material. In the isotropic case, M relates to the bulk and shear modulus (K,G) of the indented half-space by

$$M=4G\frac{3K+G}{3K+4G}. \tag{4}$$

Based on the adaptation for indentation analysis of the method of functional equations [Lee and Radok 1960], closed-form solutions for indentation in various linear viscoelastic solids became recently available for a variety of indenter shapes: flat punch indentation [Cheng et al. 2000], spherical indentation [Cheng et al. 2005; Oyen 2005], and conical indentation [Vandamme and Ulm 2006; Oyen 2006], which have been synthesized into viscoelastic indentation creep and relaxation functions for any indenter of axysmmetric shape [Vandamme and Ulm 2007]. Those linear viscoelastic approaches are relevant for materials whose behavior can be described by the classical *integer-type* time-dependent differential equation of

linear viscoelasticity [Bland 1960],

$$\sigma + \sum_{i=1}^{I} P_i \frac{d^i \sigma}{dt^i} = E'\Big(\varepsilon + \sum_{j=1}^{J} Q_j \frac{d^j \varepsilon}{dt^j}\Big), \qquad (\text{for } i = 1, 2, \dots I;\ j = 1, 2, \dots J), \tag{5}$$

where σ and ε are stress and strain, P_i and Q_j stand for relaxation and retardation time, respectively, and E' is the relaxed elasticity modulus. The restriction to integer-type time derivatives to describe the 'real' stress relaxation and creep behavior of polymers and other materials has been recognized as a drawback for material characterization [Rossikhin and Shitikova 2004] and can be removed by the introduction of fractional derivatives in the time-dependent differential equation. The application of fractional viscoelastic material models in indentation analysis is the focus of this paper. The paper is structured as follows: Following a brief review of the basic concepts of fractional derivatives, we derive a general differential representation of the time-dependent indentation response of a fractional viscoelastic material half-space using the correspondence principle. The general solution is then adapted to derive creep and relaxation functions that potentially allow the determination of meaningful viscous material properties from time-dependent experimental indentation data.

2. Elements of fractional order derivatives

Fractional calculus is an old mathematical topic, but its application in physics and engineering is more recent. For instance, in viscoelasticity and hereditary solid mechanics [Bagley and Torvik 1983], electromagnetic systems [Engheta 1996], and diffusion phenomena in inhomogeneous media [Arkhincheev 1993] , fractional order derivatives have been used to describe the system behavior. From a mathematical perspective, fractional derivatives are an extension of ordinary derivatives, and possess mathematical definitions and properties that stem from ordinary derivatives. Some definitions of fractional derivatives can be found in [Podlubny 1999] and [Kilbas et al. 2006]. The Riemann–Liouville definition is the simplest one. According to this definition, the α-th order fractional derivative of a function $f(t)$ with respect to t is

$$\mathrm{D}^{\alpha} f(t) = \frac{\partial^{\alpha}}{\partial t^{\alpha}} f(t) = \frac{1}{\Gamma(m-\alpha)} \frac{\partial^m}{\partial t^m} \int_a^t \frac{f(\tau)}{(t-\tau)^{\alpha+1-m}} d\tau, \qquad m-1 \le \alpha < m, \tag{6}$$

where m is the first integer larger than α, and a is the lower limit related to the operation of fractional differentiation. Following [Ross 1977], we call a the lower terminal value and set $a = 0$ for all fractional definitions in this article. We also use the short hand notation $D^{\alpha} f(t) = \frac{\partial^{\alpha}}{\partial t^{\alpha}} f(t)$. The Laplace transform of the Riemann–Liouville derivative is given by

$$\widehat{\mathrm{D}^{\alpha} f(t)} = s^{\alpha} \widehat{f(s)} - \sum_{k=0}^{m-1} s^k D^{\alpha-k-1} f(0), \qquad m-1 \le \alpha < m, \tag{7}$$

where s is the Laplace parameter and $\widehat{f(s)}$ stands for the Laplace transform of $f(t)$. Applying this definition to solve initial value problems requires knowledge of the non-integer derivatives of the initial conditions at $t = 0$. Despite the fact that mathematically these problems can be solved successfully, their solution is practically meaningless because there is no physical interpretation available for such

initial conditions. A solution to this conflict was proposed by Caputo [1967; 1969]. Caputo's fractional derivative (for a zero terminal value) can be written as

$$D^{\alpha} f(t) = \frac{1}{\Gamma(m-\alpha)} \int_0^t \frac{f^{(m)}(\tau)}{(t-\tau)^{\alpha+1-m}} d\tau, \qquad m-1 < \alpha < m, \tag{8}$$

where $f^{(m)}(\tau) = \frac{\partial^m}{\partial \tau^m} f(\tau)$. The Laplace transform of (8) is given by

$$\widehat{D^{\alpha} f(t)} = s^{\alpha} \widehat{f(s)} - \sum_{k=0}^{m-1} s^{\alpha-1-k} f^{(k)}(0), \qquad m-1 < \alpha \leq m, \tag{9}$$

where in (9), only ordinary derivatives are acted upon initial conditions. Another main difference between the two definitions is that the Caputo derivative (8) of a constant C is zero,

$$D^{\alpha} C = 0, \tag{10}$$

whereas in the cases of a finite lower terminal value, the Riemann–Liouville fractional derivative (6) of a constant C is not zero but is given by [Podlubny 1999]

$$\mathrm{D}^{\alpha} C = \frac{C t^{-\alpha}}{\Gamma(1-\alpha)}. \tag{11}$$

It can be shown that for $\alpha \to m$, Caputo's fractional derivative becomes a conventional m-th derivative [Podlubny 1999; Kilbas et al. 2006],

$$D^{\alpha} f(t) = f^{(m)}(t). \tag{12}$$

Similar to integer-order differentiation, Caputo's fractional differentiation is a linear operation,

$$D^{\alpha}\big(\lambda f(t) + \mu g(t)\big) = \lambda D^{\alpha} f(t) + \mu D^{\alpha} g(t), \tag{13}$$

where λ and μ are constants. Analogous to [Schiessel et al. 1995], by using Caputo's fractional derivative, the well-known Hookian spring relation, $\sigma(t) = E\varepsilon(t)$, and Newtonian dashpot relation, $\sigma(t) = \eta\, d\varepsilon(t)/dt$, can be generalized to

$$\sigma(t) = E\tau^{\alpha} \frac{d^{\alpha}\varepsilon(t)}{dt^{\alpha}} = E\tau^{\alpha} D^{\alpha}\varepsilon(t), \qquad 0 < \alpha < 1. \tag{14}$$

In (14), the parameter τ with units of time is employed to non-dimensionalize the fractional derivative of ε, which helps to obtain a meaningful physical relation between stress and strain. Note that here, since $0 < \alpha < 1$, Eq (8) reduces to

$$D^{\alpha} f(t) = \frac{1}{\Gamma(1-\alpha)} \int_0^t \frac{f^{(1)}(\tau)}{(t-\tau)^{\alpha}} d\tau, \qquad 0 < \alpha < 1. \tag{15}$$

Throughout this work, we will exclusively refer to Caputo's definition when using the term fractional derivatives. A full discussion on differences between Caputo and Riemann–Liouville fractional derivatives, and the conditions when they both become equivalent, can be found in [Podlubny 1999]. The introduction of the integrodifferential operator (15) in (14) offers a number of interesting perspectives for modeling viscoelastic behavior. From a mathematical perspective, due to the convolution with $t^{-\alpha}$, $\sigma(t)$ has a fading memory [Baker et al. 1996]. To illustrate this behavior, consider a simple rod in uniaxial

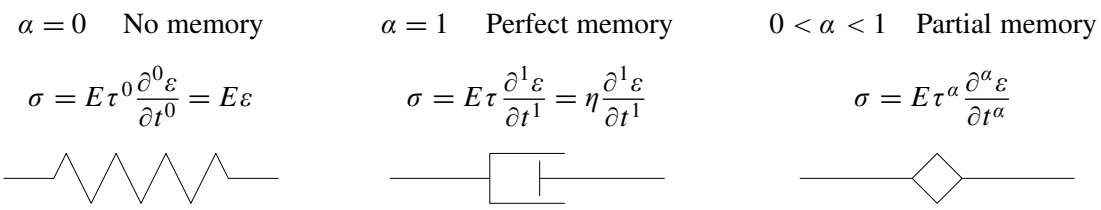

Figure 1. Illustration of integer and fractional models.

extension by a strain ε. In the limit cases, if $\alpha = 0$, $D^\alpha \varepsilon = \varepsilon$, and if $\alpha = 1$, $D^\alpha \varepsilon = \dot{\varepsilon}$ (this can be proved by integration by parts). Thus, by multiplying a constant, $E\tau^\alpha$, to $D^\alpha \varepsilon$, depending on the value of α, one obtains either the elastic force (spring model) or the damping force (dashpot model). In other words, $\alpha = 0$ corresponds to a system with no memory since the stress depends only on the instantaneous magnitude of ε (Figure 1, left), while $\alpha = 1$ corresponds to a system with perfect memory since the time history and the particular way the system has reached its current position becomes important for derivative calculations (Figure 1, middle). For any $0 < \alpha < 1$, the system has partial memory, and consequently the derived stress is a combination of dashpot and spring models (symbolized by a square in Figure 1, right). Relative to discrete (integer) derivatives, therefore, fractional derivatives offer a wide range for modeling the rate of change of the time-dependent behavior of viscoelastic materials in a continuous fashion. Figure 2 displays a simple function along with its half-derivative and first derivative, showing that fractional derivatives are usually sandwiched in between the closest lower and upper integer-derivatives. This allows one to monitor changes in a much smoother and compact fashion than offered by integer derivatives.

While spring and dashpot models can be recognized by only one material property parameter (E and η, respectively), introducing a fractional element requires three parameters, called α, τ, and E. A fractional element with only three parameters is mathematically and physically equivalent to an infinite number of simple springs and dashpots connected through a certain hierarchical arrangement [Schiessel and Blumen 1993]. Thus, capturing the continuous rate of change in time by means of integer-type models requires

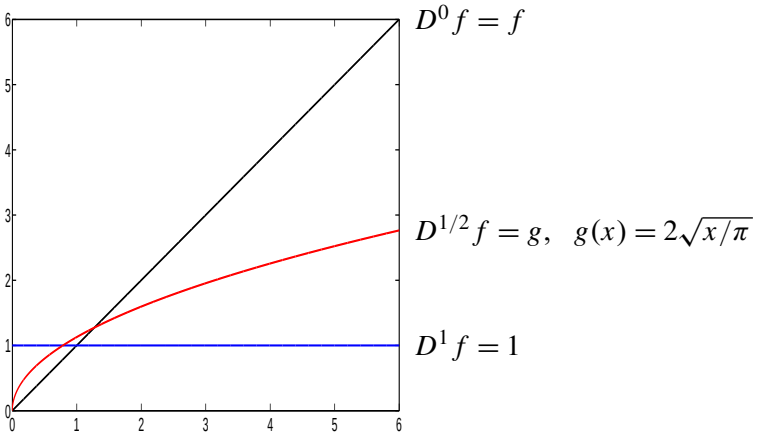

Figure 2. Derivatives of $f(x) = x$ of order 0 (black), $\frac{1}{2}$ (red) and 1 (blue).

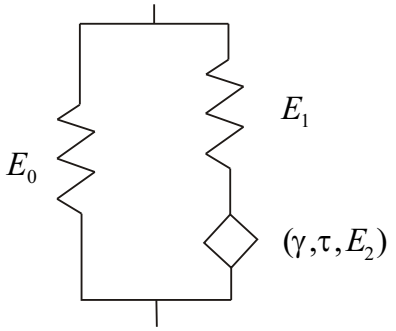

Figure 3. Fractional Zener model with identical fractional order derivatives on stress and strain.

generally many higher integer-order derivative terms in (5) to achieve a similar accuracy. With the above preliminary explanations, the extension of (5) to fractional derivatives can be written as

$$\sigma + \sum_{i=1}^{I} P_i \tau^{\alpha_i} D^{\alpha_i} \sigma = E' \Big(\varepsilon + \sum_{j=1}^{J} Q \tau^{\beta_j} D^{\beta_j} \varepsilon \Big), \qquad (\text{for } i = 1, 2, \ldots I;\ j = 1, 2, \ldots J), \tag{16}$$

where $\alpha_i, \beta_j \in [0, 1]$. Each fractional term in (16) can be considered as a replacement of a system made of many conventional springs and dashpots.

By way of application, consider a fractional Zener viscoelastic material, shown in Figure 3, in which the dashpot of the conventional Zener model is replaced by a fractional element. As shown below, this model is described by a fractional differential equation in which only the first fractional derivative terms ($I = J = 1$) are present in each series in (16), and in which the fractional derivative of stress and strain is identical ($\alpha_1 = \beta_1$). There are five independent parameters in this model, called E_0, E_1, E_2, γ, τ. Indeed, the total strain on the right branch is

$$\varepsilon = \varepsilon_s + \varepsilon_f, \tag{17}$$

where subscripts s, f refer to the spring element and the fractional element, respectively. As these elements are connected in series, their stresses are equal,

$$\sigma_R = E_1 \epsilon_s = E_2 \tau^{\gamma} D^{\gamma} \epsilon_f. \tag{18}$$

We now take advantage of the linearity property of the fractional operator (13). By taking the γ-th derivative of (17) and using (18) (assuming E_1, E_2 and τ are constants), we obtain

$$\sigma_R + \frac{E_2 \tau^{\gamma}}{E_1} D^{\gamma} \sigma_R = E_2 \tau^{\gamma} D^{\gamma} \varepsilon, \tag{19}$$

where we let

$$\tau_0 = \Big(\frac{E_2 \tau^{\gamma}}{E_1} \Big)^{1/\gamma}, \qquad S = E_2 \Big(\frac{\tau}{\tau_0} \Big)^{\gamma}. \tag{20}$$

Equation (19) simplifies to

$$\sigma_R + \tau_0^{\gamma} D^{\gamma} \sigma_R = S \tau_0^{\gamma} D^{\gamma} \varepsilon. \tag{21}$$

Equation (21), which describes the behavior of the right branch of the model in Figure 3, turns out to be the constitutive fractional differential equation of a Maxwell model in which the conventional dashpot is replaced by the fractional element.

The total stress in the parallel system is

$$\sigma = \sigma_L + \sigma_R, \tag{22}$$

where σ_L is the elastic stress in the left branch of the model displayed in Figure 3

$$\sigma_L = E_0 \varepsilon. \tag{23}$$

Then, take the γ-th derivative of (22) and multiply the result with τ_0^γ:

$$\tau_0^\gamma D^\gamma \sigma = \tau_0^\gamma D^\gamma \sigma_L + \tau_0^\gamma D^\gamma \sigma_R. \tag{24}$$

Finally, by adding (24) and (22), and using (23) and (21), we obtain

$$\sigma + \tau_0^\gamma D^\gamma \sigma = E_0 \varepsilon + (E_0 + S)\tau_0^\gamma D^\gamma \varepsilon. \tag{25}$$

Equation (25) is recognized as the one-dimensional constitutive equation of the fractional Zener model shown in Figure 3. It is characterized by identical fractional order derivatives on stress and strain. This is an important requirement for thermodynamic stability of the model described by (25).[1] More generalized constitutive equations including different fractional order derivatives on stress and strain can be found in [Schiessel et al. 1995]. In what follows, we employ the fractional Zener model in indentation analysis.

3. Time-dependent indentation response of fractional viscoelastic materials

In general, the time-dependent behavior of hereditary materials, for which the stress depends nonlineraly on the strain history, can be described by the volterra integral equations [Rabotnov 1980]. Most viscoelastic indentation solutions originate from the method of functional equations developed for linear viscoelastic contact problems by Radok [1957] and completed by Lee and Radok [1960]. The method of functional equations consists of solving the viscoelastic problem from the elastic solution by replacing the elastic moduli with their corresponding viscoelastic operators. The method of functional equations can be seen as an extension of the Laplace transform method, as formulated by Lee [1955]. The Laplace transform method consists of eliminating the explicit time dependence of the viscoelastic problem by applying the Laplace transform to the time-dependent moduli and solving the corresponding elasticity problem in the Laplace domain. The Laplace method, however, is restricted to boundary value problems in which the displacement and stress boundary conditions are fixed in time. This is generally not the case in indentation problems (except for the flat punch problem), in which the contact area changes with time, hence changing a part of the stress boundary outside the contact area into a displacement boundary inside the contact area and *vice versa*. This drawback of the Laplace transform was lifted in [Radok 1957; Lee and Radok 1960], which introduced and developed the method of functional equations, valid for linear viscoelastic problems with time-dependent boundary conditions. Galanov [1982] established

[1] There is a special case in which (25), with different fractional derivatives on stress and strain, can be thermodynamically stable. That is, when the fractional derivative acting on strain is greater than that acting on stress, and only below a certain limiting frequency [Glöckle and Nonnenmacher 1991].

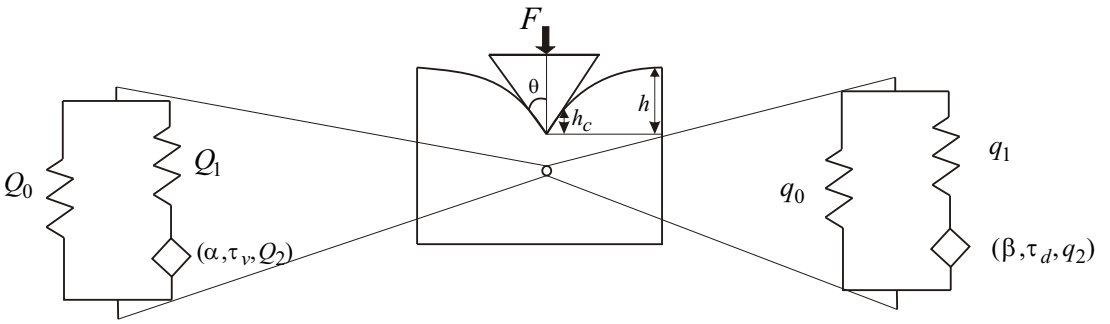

Figure 4. A rigid conical indenter on a fractional viscoelastic half-space material (middle) can be studied with a fractional Zener model describing volumetric behavior in indentation (left) or one describing deviatoric behavior in indentation (right).

self-similarity of the contact problem for some viscoelastic solids and gave dimensionless distributions for stresses under Vickers and Berkovich indenters. For indentation problems, the method of functional equations remains valid as long as the contact area (or, equivalently, for viscoelastic materials, the penetration depth) increases monotonically [Lee and Radok 1960]. We shall adopt this method for indentation analysis of fractional viscoelastic materials.

We consider the fractional Zener model shown in Figure 3, whose one-dimensional behavior is described by (25).[2] We employ this model separately for the volumetric and deviatoric part of the three-dimensional stress tensor and strain tensors of the material response to indentation. For the volumetric part with parameters Q_0, Q_1, $Q_{2,}\alpha$, τ_v, by setting, similarly to (20),

$$\zeta_v = \left(\frac{Q_2 \tau_v^\alpha}{Q_1}\right)^{1/\alpha}, \qquad K_0 = Q_2 \left(\frac{\tau_v}{\zeta_v}\right)^\alpha, \tag{26}$$

the fractional differential equation governing the time-dependent spherical isotropic material response reads (Figure 4, left),

$$\boldsymbol{\sigma}_v + \zeta_v^\alpha D^\alpha \boldsymbol{\sigma}_v = Q_0 \boldsymbol{\varepsilon}_v + (Q_0 + K_0)\zeta_v^\alpha D^\alpha \boldsymbol{\varepsilon}_v, \tag{27}$$

where $\boldsymbol{\sigma}_v = \frac{1}{3}(\operatorname{tr}\boldsymbol{\sigma})\mathbf{1}$, $\boldsymbol{\varepsilon}_v = \frac{1}{3}(\operatorname{tr}\boldsymbol{\varepsilon})\mathbf{1}$, are the volumetric parts of the second order stress tensor $\boldsymbol{\sigma}$ and second order strain tensor $\boldsymbol{\varepsilon}$, respectively. Similarly, for the deviatoric part with parameters q_0, $q_{1,}q_2$, β, τ_d, by setting

$$\zeta_d = \left(\frac{q_2 \tau_d^\beta}{q_1}\right)^{1/\beta}, \qquad G_0 = q_2 \left(\frac{\tau_d}{\zeta_d}\right)^\beta, \tag{28}$$

the fractional differential equation governing the time-dependent deviatoric isotropic material response reads (Figure 4, right)

$$\boldsymbol{\sigma}_d + \zeta_d^\beta D^\beta \boldsymbol{\sigma}_d = q_0 \boldsymbol{\varepsilon}_d + (q_0 + G_0)\zeta_d^\beta D^\beta \boldsymbol{\varepsilon}_d. \tag{29}$$

Here $\boldsymbol{\sigma}_d$ and $\boldsymbol{\varepsilon}_d$ are, respectively, the deviatoric parts of the second order stress and strain tensors, $\boldsymbol{\sigma}$ and $\boldsymbol{\varepsilon}$. From basic tensor algebra, relations $\boldsymbol{\sigma} = \boldsymbol{\sigma}_v + \boldsymbol{\sigma}_d$, $\boldsymbol{\varepsilon} = \boldsymbol{\varepsilon}_v + \boldsymbol{\varepsilon}_d$ hold. Thus, as Figure 4 shows, based

[2]For a general nonlinear stress-strain behavior in solids, the fraciotnal calculus can be integrated into the volterra equations [Rabotnov 1980].

on our chosen models, there are in total 10 independent parameters Q_0, Q_1, $Q_{2,}\alpha$, τ_v, q_0, $q_{1,}q_2$, β, τ_d that describe the volumetric and deviatoric material behavior (five for each behavior). For simplicity in notation and avoiding carrying too many parameters in our analytical derivations, we rewrite (27) and (29) as

$$\boldsymbol{\sigma}_v(t) + P D^{\alpha}\boldsymbol{\sigma}_v(t) = Q_0\boldsymbol{\varepsilon}_v(t) + Q D^{\alpha}\boldsymbol{\varepsilon}_v(t), \tag{30}$$

$$\boldsymbol{\sigma}_d(t) + p D^{\beta}\boldsymbol{\sigma}_d(t) = q_0\boldsymbol{\varepsilon}_d(t) + q D^{\beta}\boldsymbol{\varepsilon}_d(t), \tag{31}$$

where we let

$$P = \zeta_v^{\alpha}, \qquad Q = (Q_0 + K_0)\zeta_v^{\alpha}, \tag{32}$$

$$p = \zeta_d^{\beta}, \qquad q = (q_0 + G_0)\zeta_d^{\beta}. \tag{33}$$

Using (9), the Laplace transforms of (30) and (31) are readily obtained:

$$\begin{aligned}(1 + Ps^{\alpha})\widehat{\boldsymbol{\sigma}_v(s)} - Ps^{\alpha-1}\boldsymbol{\sigma}_v(0) &= (Q_0 + Qs^{\alpha})\widehat{\boldsymbol{\varepsilon}_v(s)} - Qs^{\alpha-1}\boldsymbol{\varepsilon}_v(0),\\ (1 + ps^{\beta})\widehat{\boldsymbol{\sigma}_d(s)} - ps^{\beta-1}\boldsymbol{\sigma}_d(0) &= (q_0 + qs^{\beta})\widehat{\boldsymbol{\varepsilon}_d(s)} - qs^{\beta-1}\boldsymbol{\varepsilon}_d(0),\end{aligned} \tag{34}$$

where $\widehat{\boldsymbol{\sigma}_v(s)}$, $\widehat{\boldsymbol{\sigma}_d(s)}$, $\widehat{\boldsymbol{\varepsilon}_v(s)}$, $\widehat{\boldsymbol{\varepsilon}_d(s)}$ denote the Laplace transforms of $\boldsymbol{\sigma}_v(t)$, $\boldsymbol{\sigma}_v(t)$, $\boldsymbol{\varepsilon}_v(t)$, $\boldsymbol{\varepsilon}_d(t)$, whereas $\boldsymbol{\sigma}_v(0)$, $\boldsymbol{\sigma}_d(0)$, $\boldsymbol{\varepsilon}_v(0)$, $\boldsymbol{\varepsilon}_d(0)$ represent the stress and strain initial conditions at $t = 0$. We remind ourselves of the classical Laplace transformations of the stress convolution integrals of linear isotropic viscoelasticity [Christensen 1971]:

$$\begin{aligned}\boldsymbol{\sigma}_v(t) &= \int_{-\infty}^{t} 3K(t-\tau)\frac{d}{d\tau}\boldsymbol{\varepsilon}_v(\tau)d\tau \to \widehat{\boldsymbol{\sigma}_v(s)} = 3s\widehat{K(s)}\widehat{\boldsymbol{\varepsilon}_v(s)},\\ \boldsymbol{\sigma}_d(t) &= \int_{-\infty}^{t} 2G(t-\tau)\frac{d}{d\tau}\boldsymbol{\varepsilon}_d(\tau)d\tau \to \widehat{\boldsymbol{\sigma}_d(s)} = 2s\widehat{G(s)}\widehat{\boldsymbol{\varepsilon}_d(s)},\end{aligned} \tag{35}$$

where $K(t)$ and $G(t)$ are the time-dependent bulk and shear modulus, respectively. Then, by comparing (34) and (35), one obtains the following relations for bulk and shear response of the fractional material:

$$3s\widehat{K(s)} = \frac{Q_0 + Qs^{\alpha}}{1 + Ps^{\alpha}}, \qquad 2s\widehat{G(s)} = \frac{q_0 + qs^{\beta}}{1 + ps^{\beta}}, \tag{36}$$

and

$$P\boldsymbol{\sigma}_v(0) = Q\boldsymbol{\varepsilon}_v(0), \qquad p\boldsymbol{\sigma}_d(0) = q\boldsymbol{\varepsilon}_d(0). \tag{37}$$

Equations (37) indicate that the initial conditions acting upon stress and strain are not completely independent, and relations such as (37) must be satisfied. These constraints do not appear only in fractional viscoelastic models. Analogous constraints on initial conditions also exist for integer-order viscoelastic models [Christensen 1971; Shahsavari and Ostoja-Starzewski 2005].

Similarly, application of the correspondence principle to the elastic indentation modulus M defined by (4) yields [Vandamme and Ulm 2006]

$$M \to s\widehat{M(s)} = 4s\widehat{G(s)}\frac{3s\widehat{K(s)} + s\widehat{G(s)}}{3s\widehat{K(s)} + 4s\widehat{G(s)}}. \tag{38}$$

Next, analogously to (35), the application of the correspondence principle of viscoelasticity to the elastic indentation force relation (2) yields

$$F(t) = \phi \int_{-\infty}^{t} M(t-\tau) \frac{d}{d\tau} h^{1+1/n}(\tau)\, d\tau \quad \Longrightarrow \quad \widehat{F(s)} = \phi s \widehat{M(s)}\ \widehat{h^{1+1/n}(s)}. \tag{39}$$

In (39), we a priori assumed the geometry parameter ϕ is a time-independent parameter, following [Lee and Radok 1960]. By substituting (36) in (38) and then in (39), one obtains the viscoelastic relation between $\widehat{F(s)}$ and $\widehat{h^{1+1/n}}$ in the transformed Laplace space. Next, by extensively rearranging the terms and using the relation (9) along with the linearity property (13) for the fractional order terms, the constitutive differential equation governing the time-dependent indentation response becomes

$$D_F(F(t)) = 2\phi D_h(h^{1+1/n}(t)). \tag{40}$$

This is a differential equation with constant coefficients involving the operators

$$\begin{aligned} D_F &= c_0 + c_1 D^{\alpha} + c_2 D^{\beta} + c_3 D^{\alpha+\beta} + c_4 D^{\alpha+2\beta} + c_5 D^{2\beta}, \\ D_h &= l_0 + l_1 D^{\alpha} + l_2 D^{\beta} + l_3 D^{\alpha+\beta} + l_4 D^{\alpha+2\beta} + l_5 D^{2\beta} \end{aligned} \tag{41}$$

with coefficients

$$\begin{aligned} c_0 &= Q_0 + 2q_0, & l_0 &= \tfrac{1}{2} q_0^2 + q_0 Q_0, \\ c_1 &= Q + 2Pq_0, & l_1 &= q_0 Q + \tfrac{1}{2} P q_0^2, \\ c_2 &= 2Q_0 p + 2q + 2pq_0, & l_2 &= q_0 p Q_0 + q q_0 + q Q_0, \\ c_3 &= 2Qp + 2Pq + 2Ppq_0, & l_3 &= q_0 p Q + P q q_0 + q Q, \\ c_4 &= Qp^2 + 2Ppq, & l_4 &= qpQ + \tfrac{1}{2} P q^2, \\ c_5 &= Q_0 p^2 + 2pq, & l_5 &= qpQ_0 + \tfrac{1}{2} q^2. \end{aligned} \tag{42}$$

Note that in view of (37) the following relations between initial conditions hold:

$$c_i F(0) = 2\phi l_i \Omega(0), \qquad (i = 1, 2, \ldots, 5), \tag{43}$$

$$c_i F^{(1)}(0) = 2\phi l_i \Omega^{(1)}(0), \qquad (i = 3, 4, 5), \tag{44}$$

$$c_4 F^{(2)}(0) = 2\phi l_4 \Omega^{(2)}(0), \tag{45}$$

where we have set $\Omega(0) = h^{1+1/n}\ (0)$. Considering the initial conditions above, the use of Caputo's derivative results in five integer-order relations in (43) and four inter-order derivatives in (44) and (45). In order for (44) to hold with $i = 3$, we must have $\alpha + \beta > 1$; the same relation with $i = 4$ and $i = 5$ requires $\alpha + 2\beta > 1$ and $2\beta > 1$, respectively. Similarly, (45) requires that $\alpha + 2\beta > 2$. If any of these conditions is not met, the corresponding relation in (44)–(45) does not exist.

The following observations deserve attention:

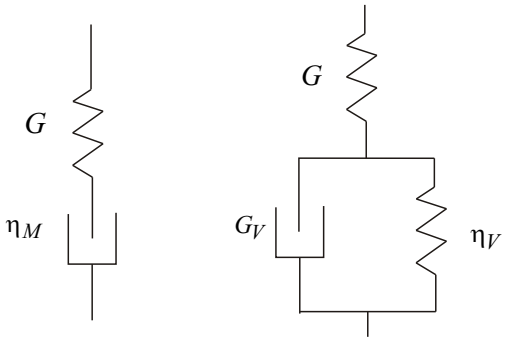

Figure 5. Left: Maxwell model. Right: Zener model.

(i) For $\alpha = \beta = 0$, which corresponds to the case of a material with no memory (Figure 1, left), Equation (40) reduces to the elastic indentation relation (2), with

$$M = \frac{2l_0}{c_0} = 2q_0 \frac{Q_0 + \frac{1}{2}q_0}{Q_0 + 2q_0}, \qquad K = \frac{1}{3}Q_0, \qquad G = \frac{1}{2}q_0. \tag{46}$$

(ii) Letting $\alpha = 0$ corresponds to the case of a pure deviatoric creep, a case which was extensively studied in integer-type viscoelastic indentation analysis (for example, [Cheng and Cheng 2004; Cheng et al. 2000; 2005; Vandamme and Ulm 2006]). In this case $\beta = 1$, and one obtains

$$\big(c_0 + (c_2 + c_3)D^1 + (c_4 + c_5)D^2\big)F(t) = 2\phi\big(l_0 + (l_2 + l_3)D^1 + (l_4 + l_5)D^2\big)h^{1+1/n}(t). \tag{47}$$

Note that a deviatoric creep behavior described at a material level by a *first*-order differential equation (see (31) for $\beta = 1$), yields a *second*-order differential equation that governs the $F(t) - h(t)$ indentation response. This includes, as integer subset models, the three-parameter deviator creep Maxwell model and the four-parameter deviator creep Kelvin–Voigt or Zener model (Figure 5), for which the constant coefficients read as follows:

	P	Q_0	Q	p	q_0	q
Maxwell	0	$3K$	0	η_M/G	0	$2\eta_M$
Zener	0	$3K$	0	$\dfrac{\eta_V}{G+G_V}$	$2\dfrac{GG_V}{G+G_V}$	$2\dfrac{G}{G+G_V}\eta_V$

(48)

Here η_M and η_V stand for the viscosity in the respective models. Use of (48) in (42) and then in (47) yields the following differential equations for the two particular integer-type viscoelastic models:

$$\text{Maxwell: } F(t) + \frac{c_2}{c_0}\frac{\partial F}{\partial t} + \frac{c_5}{c_0}\frac{\partial^2 F}{\partial t^2} = 2\phi\Big(\frac{l_2}{c_0}\frac{\partial h^{1+1/n}}{\partial t} + \frac{l_5}{c_0}\frac{\partial^2 h^{1+1/n}}{\partial t^2}\Big), \tag{49}$$

$$\text{Zener: } F(t) + \frac{c_2}{c_0}\frac{\partial F}{\partial t} + \frac{c_5}{c_0}\frac{\partial^2 F}{\partial t^2} = 2\frac{l_0}{c_0}\phi\Big(h^{1+1/n} + \frac{l_2}{l_0}\frac{\partial h^{1+1/n}}{\partial t} + \frac{l_5}{l_0}\frac{\partial^2 h^{1+1/n}}{\partial t^2}\Big). \tag{50}$$

(iii) The difference in differential order between the material and the indentation scale becomes even more apparent for $\alpha = \beta = 1$, which converts the fractional model into an integer-type model governed

by a third-order differential equation:

$$\big(c_0+(c_1{+}c_2)D^1+(c_3{+}c_5)D^2+c_4D^3\big)F(t) = 2\phi\big(l_0+(l_1{+}l_2)D^1+(l_3{+}l_5)D^2+l_4D^3\big)h^{1+1/n}(t). \quad (51)$$

Setting $\alpha = \beta$ reduces the model to the often considered case of a material with time independent Poisson's ratio [Gao and Ogden 2003], which is obtained by letting $P = p$, $q = bQ$, and $q_0 = bQ_0$ for any non-negative value of b in (30)–(31) and (42). This concept is similar to using two same-type integer viscoelastic models with the aforementioned relations between their parameters which lead to a constant Poisson's ratio [Tschoegl et al. 2002].

(iv) This difference in differential order between the material and the indentation scale holds true for fractional materials; that is, because of the definition of the differential operators in (41), the order of the fractional derivatives at the indentation scale given by (40), is always greater than the one of the material level defined by (30)–(31). For example, for a deviatoric fractional creep model, $\alpha = 0$, the differential equation (31) governing the material behavior is of order $0 < \beta < 1$, while the indentation response is of order 2β, and can thus be greater than unity:

$$\big(c_0+(c_2{+}c_3)D^{\beta}+(c_4{+}c_5)D^{2\beta}\big)F(t) = 2\phi\big(l_0+(l_2{+}l_3)D^{\beta}+(l_4{+}l_5)D^{2\beta}\big)h^{1+1/n}(t). \quad (52)$$

The specification of (52) for a fractional deviatoric Maxwell material ($P = Q = q_0 = 0$) and a fractional deviatoric Zener material ($P = Q = 0$) reads as follows:

$$\text{Maxwell: } F(t)+\frac{c_2}{c_0}\frac{\partial^{\beta}F}{\partial t^{\beta}}+\frac{c_5}{c_0}\frac{\partial^{2\beta}F}{\partial t^{2\beta}} = 2\phi\Big(\frac{l_2}{c_0}\frac{\partial^{\beta}h^{1+1/n}}{\partial t^{\beta}}+\frac{l_5}{c_0}\frac{\partial^{2\beta}h^{1+1/n}}{\partial t^{2\beta}}\Big), \quad (53)$$

$$\text{Zener: } F(t)+\frac{c_2}{c_0}\frac{\partial^{\beta}F}{\partial t^{\beta}}+\frac{c_5}{c_0}\frac{\partial^{2\beta}F}{\partial t^{2\beta}} = 2\frac{l_0}{c_0}\phi\Big(h^{1+1/n}+\frac{l_2}{l_0}\frac{\partial^{\beta}h^{1+1/n}}{\partial t^{\beta}}+\frac{l_5}{l_0}\frac{\partial^{2\beta}h^{1+1/n}}{\partial t^{2\beta}}\Big), \quad (54)$$

where the coefficients $c_0, \ldots, c_5$ and $l_0, \ldots, l_5$) are still given by (42). Their dimensionality, however, changes due to the application of non-integer time derivatives. For instance, we have $[c_2/c_0] = [l_2/l_0] = T^{\beta}$, while $[c_5/c_0] = [l_5/l_0] = T^{2\beta}$, and so on. Still, analogously to (19)–(20), one can define parameters similar to τ_0 with the dimension of time and replace the the fractional dimension of c_2/c_0, etc.

(v) The operators (41) are not symmetric with respect to α and β; that is, in contrast to α, which is the fractional exponent for the volumetric viscoelastic response (30), there are some extra terms that involve higher derivatives of order 2β, which is the fractional exponent for the viscoelastic shear response (31). This observation translates, into fractional derivatives, the well-known fact that an indentation test is a shear test than a hydrostatic test. For this reason, the effect of β dominates over the effect of α in the fractional derivatives that define the indentation response (40). This dominance of shear over bulk exists for conventional viscoelastic materials in indentation, but it is hidden in the constitutive equations.

4. Indentation creep and relaxation functions

A convenient way to analyze time-dependent experimental indentation data is in the form of indentation creep and relaxation functions, derived for a step force loading or step displacement loading, respectively. It is also a formidable illustration of the use of the fractional model developed here before.

4.1. ***Indentation creep compliance.*** Consider a Heaviside step loading $F(t) = F_{\max}\mathcal{H}(t)$, where $F_{\max}$ is the maximum load, and $\mathcal{H}(t)$ the Heaviside step function. We recall the Laplace transform $\widehat{F(s)}$ of the Heaviside load function:

$$F(t) = F_{\max}\mathcal{H}(t) \quad \Longleftrightarrow \quad \widehat{F(s)} = \frac{F_{\max}}{s}. \tag{55}$$

Then, a substitution of (55) in (39) along with a substitution of (55) in Laplace transform of (40) can be developed in the form

$$\widehat{L(s)} = \frac{\phi\widehat{h^{1+1/n}(s)}}{F_{\max}} = \frac{1}{s^2\widehat{M(s)}} = \frac{\widehat{D_F(s)}}{2s\widehat{D_h(s)}}, \tag{56}$$

where $D_F(s)$ and $D_h(s)$ are the Laplace transforms of the operators (41) according to definition (9):[3]

$$\widehat{D_F(s)} = c_0 + c_1 s^{\alpha} + c_2 s^{\beta} + c_3 s^{\alpha+\beta} + c_4 s^{\alpha+2\beta} + c_5 s^{2\beta}, \tag{57}$$

$$\widehat{D_h(s)} = l_0 + l_1 s^{\alpha} + l_2 s^{\beta} + l_3 s^{\alpha+\beta} + l_4 s^{\alpha+2\beta} + l_5 s^{2\beta}. \tag{58}$$

Note that the inverse Laplace transform of (56), $L(t)$, has dimension of compliance $[L] = 1/(L^{-1}MT^{-2})$, and can therefore be appropriately called an indentation creep compliance function. As discussed in detail for integer-type viscoelasticity models in [Vandamme and Ulm 2007], the indentation creep compliance is independent of the indenter-shape. The right-hand side of (56), therefore, is representative of the material response of the considered fractional viscoelastic material. The inverse transform of (56) exists, is real, and continuous. The following statements are derived in the Appendix:

(i) For a 'double' Zener model (Zener bulk and Zener deviatoric creep model), the inverse Laplace transform of (56) yields the following expression of the time-dependent indentation creep compliance:

$$\begin{aligned} L(t) &= \frac{\phi h^{1+1/n}(t)}{F_{\max}} \\ &= \frac{c_0}{2l_0} + \frac{1}{\pi}\operatorname{Im}\int_0^{\infty} \frac{\widehat{D_F(re^{-i\pi})}}{2re^{-i\pi}\widehat{D_h(re^{-i\pi})}} \exp(-rt)\,dr + \sum_j \lim_{s\to\lambda_j^m}(s-\lambda_j^m)\frac{\widehat{D_F(\lambda_j^m)}\exp(\lambda_j^m t)}{2\lambda_j^m\widehat{D_h(\lambda_j^m)}}, \end{aligned} \tag{59}$$

where m is the smallest common denominator of the fractional numbers α and β. Note that λ^m is a complex number with negative real part. Thus, as $t \to \infty$, the second and the third terms on the right-hand side of (59) vanish and $L(t)$ converges to a constant $c_0/2l_0$. This is because in Zener-type models (either fractional or integer; see Figure 5, right), there is a spring parallel to the rest of the system that prevents infinite deformation.

[3]Initial conditions in the Laplace transform of a derivative of a Heaviside function are zero, since 0^- (and not 0^+) is taken as a lower limit of Laplace integration for a Heaviside function. More details can be found in [Flügge 1967].

(ii) For a 'double' Maxwell model, the expression of the inverse Laplace transform is the same one as (59), except for the first term on the right:

$$L(t) = \frac{\phi h^{1+1/n}(t)}{F_{\max}}$$
$$= \frac{1}{2(k-1)!}\ \frac{\partial^{k-1}}{\partial u^{k-1}}[f(u)\exp(u^m t)]_{u=0} + \frac{1}{\pi}\operatorname{Im}\int_0^\infty \frac{\widehat{D_F(re^{-i\pi})}}{2re^{-i\pi}\,\widehat{D_h(re^{-i\pi})}}\exp(-rt)\,dr$$
$$+\sum_j \lim_{s\to\lambda_j^m}(s-\lambda_j^m)\frac{\widehat{D_F(\lambda_j^m)}\exp(\lambda_j^m t)}{2\lambda_j^m\,\widehat{D_h(\lambda_j^m)}}, \quad (60)$$

where $k = m(1+\beta)$ is an integer, and

$$f(u) = \frac{c_1 + c_2u^{m(\beta-\alpha)} + c_3u^{m\beta} + c_4u^{2m\beta} + c_5u^{m(2\beta-\alpha)}}{2(l_3 + l_4u^{m\beta} + l_5u^{m(\beta-\alpha)})}, \quad \alpha \le \beta,$$
$$f(u) = \frac{c_1u^{m(\alpha-\beta)} + c_2 + c_3u^{m\alpha} + c_4u^{m(\alpha+\beta)} + c_5u^{m\beta}}{2(l_3u^{m(\alpha-\beta)} + l_4u^{m\alpha} + l_5)}, \quad \alpha > \beta. \quad (61)$$

Specification of (60) for a fractional deviatoric Maxwell material ($P = Q = q_0 = 0, \alpha = 0$) and of (59) for a fractional deviatoric Zener material ($P = Q = 0, \alpha = 0$) yields

$$\text{Maxwell: } L(t) = \frac{1}{2(k-1)!}\frac{\partial^{k-1}}{\partial u^{k-1}}\left[\frac{Q_0 + (2Q_0p+2q)u^{m\beta} + (Q_0p^2+2pq)u^{2m\beta}}{qQ_0 + (qpQ_0 + \frac{1}{2}q^2)u^{m\beta}}\exp(u^m t)\right]_{u=0}$$
$$+\frac{1}{\pi}\operatorname{Im}\int_0^\infty \frac{Q_0 + (2Q_0p+2q)r^\beta e^{-i\pi\beta} + (Q_0p^2+2pq)r^{2\beta}e^{-2i\pi\beta}}{2r^{1+\beta}e^{-i\pi(1+\beta)}\big(qQ_0 + (qpQ_0+\frac{1}{2}q^2)r^\beta e^{-i\pi\beta}\big)}\exp(-rt)\,dr$$
$$+\sum_j \lim_{s\to\lambda_j^m}(s-\lambda_j^m)\frac{Q_0 + (2Q_0p+2q)\lambda_j^{\beta m} + (Q_0p^2+2pq)\lambda_j^{2\beta m}}{2\lambda_j^{m(1+\beta)}\big(qQ_0 + (qpQ_0+\frac{1}{2}q^2)s^\beta\big)}\exp\big(\lambda_j^m t\big), \quad (62)$$

$$\text{Zener: } L(t) = \frac{\frac{1}{2}Q_0 + q_0}{\frac{1}{2}q_0^2 + q_0Q_0}$$
$$+\frac{1}{\pi}\operatorname{Im}\int_0^\infty \frac{\big(Q_0 + 2q_0 + (2Q_0p + 2q + 2pq_0)r^\beta e^{-i\pi\beta} + (Q_0p^2+2pq)r^{2\beta}e^{-2i\pi\beta}\big)\exp(-rt)}{2re^{-i\pi}\big(\frac{1}{2}q_0^2 + q_0Q_0 + (q_0pQ_0 + qq_0 + qQ_0)r^\beta e^{-i\pi\beta} + (qpQ_0+\frac{1}{2}q^2)r^{2\beta}e^{-2i\pi\beta}\big)}\,dr$$
$$+\sum_j \lim_{s\to\lambda_j^m}\big(s-\lambda_j^m\big)\frac{Q_0 + 2q_0 + (2Q_0p + 2q + 2pq_0)\lambda_j^{\beta m} + (Q_0p^2+2pq)\lambda_j^{2\beta m}}{2\lambda_j^m\big(\frac{1}{2}q_0^2 + q_0Q_0 + (q_0pQ_0 + qq_0 + qQ_0)s^\beta + (qpQ_0+\frac{1}{2}q^2)s^{2\beta}\big)}\exp(\lambda_j^m t). \quad (63)$$

(iii) For $\beta = 1$, since $e^{-i\pi} = -1$, the imaginary part of the integrand in the middle terms of both (62) and (63) become zero and hence the middle terms vanish. In this case, the other two terms in (62) and (63) are found to reduce to the known indentation creep compliance functions of the integer-type deviatoric models as follows [Vandamme and Ulm 2007]:

$$\text{Maxwell: } L(t) = \frac{1}{M} + \frac{t}{4\eta_M} + \frac{(1-2\nu)^2}{4E}\left(1 - \exp\Big(-\frac{E}{3\eta_M}t\Big)\right), \quad (64)$$

$$\text{Zener: } L(t) = \frac{1}{M} + \frac{1}{4G_V}\left(1 - \exp\Big(-\frac{G_V}{\eta_V}t\Big)\right) + \frac{(1-2\nu)^2}{4(E+3G_V)}\left(1 - \exp\Big(-\frac{E+3G_V}{3\eta_V}t\Big)\right). \quad (65)$$

Here we have used the notation (42) and (42) along with the well known elasticity relations

$$E = \frac{9KG}{3K+G}, \qquad \nu = \frac{3K-2G}{2(3K+G)}.$$

(iv) Finally, the indentation creep compliance function can be used to study the time-dependent indentation response $h(t)$ for any prescribed monotonically increasing indentation load history $F(t) = F_{max}\mathscr{F}(t)$, in both the Laplace and time domain [Vandamme and Ulm 2007]:

$$\frac{\phi\widehat{h^{1+1/n}}(s)}{F_{\max}} = s\widehat{L(s)}\widehat{\mathscr{F}(s)} \quad \Longrightarrow \quad \frac{\phi h^{1+1/n}(t)}{F_{\max}} = \int_{-\infty}^{t} L(t-\tau)\frac{d}{d\tau}\mathscr{F}(\tau)d\tau, \tag{66}$$

where $\widehat{\mathscr{F}(s)}$ is the Laplace transform of the normalized loading history $\mathscr{F}(t) = F(t)/F_{\max}$, satisfying $(d\mathscr{F}/dt)(t) \geq 0$.

4.2. ***Indentation relaxation modulus.*** For a Heaviside displacement loading $h^{1+1/n}(t) = h_{\max}^{1+1/n}\mathscr{H}(t)$, one can principally proceed in a similar way as for the indentation creep compliance. Alternatively, one can make use of the link between indentation creep compliance $L(t)$ and indentation relaxation modulus $M(t)$, given by (see [Vandamme and Ulm 2007])

$$(s\widehat{M(s)})^{-1} = s\widehat{L(s)}. \tag{67}$$

The expression of the relaxation modulus in the Laplace space thus becomes

$$\widehat{M(s)} = \frac{\widehat{F(s)}}{\phi h_{\max}^{1+1/n}} = \frac{1}{s^2\widehat{L(s)}} = \frac{2\widehat{D_h(s)}}{s\widehat{D_F(s)}}. \tag{68}$$

The inverse Laplace transform for a selected number of models are as follows:

(i) For the 'double' Zener material:

$$M(t) = \frac{F(t)}{\phi h_{\max}^{1+1/n}} = \frac{2l_0}{c_0} + \frac{1}{\pi}\operatorname{Im}\int_0^{\infty} \frac{2\widehat{D_h(s)}}{s\widehat{D_F(s)}}\exp(-rt)\,dr + \sum_j \left(s-\lambda_j^m\right)\frac{2\widehat{D_h\left(\lambda_j^m\right)}\exp\left(\lambda_j^m t\right)}{\lambda_j^m\widehat{D_F\left(\lambda_j^m\right)}}. \tag{69}$$

(ii) For the 'double' Maxwell material:

$$\begin{aligned} M(t) = \frac{F(t)}{\phi h_{\max}^{1+1/n}} &= \frac{1}{(k-1)!}\frac{\partial^{k-1}}{\partial u^{k-1}}[f(u)\exp(u^m t)]_{u=0} \\ &+ \frac{1}{\pi}\operatorname{Im}\int_0^{\infty} \frac{2\widehat{D_h(re^{-i\pi})}}{re^{-i\pi}\widehat{D_F(re^{-i\pi})}}\exp(-rt)\,dr + \sum_j \left(s-\lambda_j^m\right)\frac{2\widehat{D_F\left(\lambda_j^m\right)}\exp\left(\lambda_j^m t\right)}{2\lambda_j^m\widehat{D_h\left(\lambda_j^m\right)}}, \end{aligned} \tag{70}$$

where $k = m(1-\beta)$ is an integer, and

$$\begin{aligned} f(u) &= \frac{2(l_3 + l_4u^{m\beta} + l_5u^{m(\beta-\alpha)})}{c_1 + c_2u^{m(\beta-\alpha)} + c_3u^{m\beta} + c_4u^{2m\beta} + c_5u^{m(2\beta-\alpha)}}, \quad \alpha \leq \beta, \\ f(u) &= \frac{2(l_3u^{m(\alpha-\beta)} + l_4u^{m\alpha} + l_5)}{c_1u^{m(\alpha-\beta)} + c_2 + c_3u^{m\alpha} + c_4u^{m(\alpha+\beta)} + c_5u^{m\beta}}, \quad \alpha > \beta. \end{aligned} \tag{71}$$

The relaxation moduli for fractional deviatoric Maxwell and Zener materials are, respectively,

$$M(t)=\frac{1}{(k-1)!}\frac{\partial^{k-1}}{\partial u^{k-1}}\left[\frac{Q_0+(2Q_0p+2q)u^{m\beta}+(Q_0p^2+2pq)u^{2m\beta}}{qQ_0+(qpQ_0+\frac{1}{2}q^2)u^{m\beta}}\exp(u^m t)\right]_{u=0}$$
$$+\frac{1}{\pi}\operatorname{Im}\int_0^\infty \frac{2\big(Q_0+(2Q_0p+2q)r^\beta e^{-i\pi\beta}+(Q_0p^2+2pq)r^{2\beta}e^{-2i\pi\beta}\big)}{r^{1+\beta}e^{-i\pi(1+\beta)}\big(qQ_0+(qpQ_0+\frac{1}{2}q^2)r^\beta e^{-i\pi\beta}\big)}\exp(-rt)\,dr$$
$$+\sum_j \lim_{s\to\lambda_j^m}(s-\lambda_j^m)\frac{2\big(Q_0+(2Q_0p+2q)\lambda_j^{\beta m}+(Q_0p^2+2pq)\lambda_j^{2\beta m}\big)}{\lambda_j^{m(1+\beta)}\big(qQ_0+(qpQ_0+\frac{1}{2}q^2)s^\beta\big)}\exp(\lambda_j^m t), \quad (72)$$

$$M(t)=\frac{\frac{1}{2}q_0^2+q_0Q_0}{\frac{1}{2}Q_0+q_0}$$
$$+\frac{1}{\pi}\operatorname{Im}\int_0^\infty \frac{2\big(\frac{1}{2}q_0^2+q_0Q_0+(q_0pQ_0+qq_0+qQ_0)r^\beta e^{-i\pi\beta}+(qpQ_0+\frac{1}{2}q^2)r^{2\beta}e^{-2i\pi\beta}\big)\exp(-rt)}{re^{-i\pi}\big(Q_0+2q_0+(2Q_0p+2q+2pq_0)r^\beta e^{-i\pi\beta}+(Q_0p^2+2pq)r^{2\beta}e^{-2i\pi\beta}\big)}\,dr$$
$$\sum_j \lim_{s\to\lambda_j^m}(s-\lambda_j^m)\frac{2\big(\frac{1}{2}q_0^2+q_0Q_0+(q_0pQ_0+qq_0+qQ_0)\lambda_j^{\beta m}+(qpQ_0+\frac{1}{2}q^2)\lambda_j^{2\beta m}\big)\exp(\lambda_j^m t)}{\lambda_j^m\big(Q_0+2q_0+(2Q_0p+2q+2pq_0)s^\beta+(Q_0p^2+2pq)s^{2\beta}\big)}, \quad (73)$$

Similar to creep compliances, for $\beta=1$, the previous expressions are found to reduce to the known indentation relaxation modulus expressions of the integer-type deviatoric models [Vandamme and Ulm 2007]:

$$\text{Maxwell: } M(t)=M-\frac{E}{2(1+\nu)}(1-e^{-\frac{E}{2(1+\nu)\eta_M}t})-\frac{E}{2(1-\nu)}\left(1-\exp\Big(-\frac{E}{6(1-\nu)\eta_M}t\Big)\right), \quad (74)$$

$$\text{Zener: } M(t)=M-\frac{E^2}{2(1+\nu)(E+2G(1+\nu))}\left(1-\exp\Big(-\frac{(E+2G(1+\nu))t}{2\eta_V(1+\nu)}\Big)\right)$$
$$-\frac{E^2}{2(1-\nu)(E+6G(1-\nu))}\left(1-\exp\Big(-\frac{(E+6G(1-\nu))t}{6\eta_V(1-\nu)}\Big)\right). \quad (75)$$

The indentation relaxation modulus functions can be used to study the time-dependent force relaxation history $F(t)$ for any prescribed monotonically increasing indentation displacement history $h^{1+1/n}(t)=h_{max}^{1+1/n}\mathcal{G}(t)$, in both Laplace and time domain [Vandamme and Ulm 2007]:

$$\frac{\widehat{F(s)}}{\phi h_{\max}^{1+1/n}}=s\widehat{M(s)}\widehat{\mathcal{G}(s)} \quad\Longrightarrow\quad \frac{F(t)}{\phi h_{\max}^{1+1/n}}=\int_{-\infty}^{t}M(t-\tau)\frac{d}{d\tau}\mathcal{G}(\tau)d\tau, \quad (76)$$

where $\widehat{\mathcal{G}(s)}$ is the Laplace transform of $\mathcal{G}(t)=h^{1+1/n}(t)/h_{\max}^{1+1/n}$, the normalized displacement loading history, which satisfies $(d\mathcal{G}/dt)(t)\geq 0$.

5. Application

In this section, we illustrate the application of the above theoretical derivations in indentation analysis of the fractional and viscous parameters of polystyrene (Dupont, Wilmington, DE) under a creep test. Depth-sensing indentation experiment was performed with a Nanotest 600 nanoindenter (MicroMaterials Ltd., Wrexham) with a Berkovich indenter. As is common practice in indentation analysis, the Berkovich

Maximum force [mN]	500	Thermal drift [nm/sec]	< 0.1
Load resolution [nN]	2–3	Machine compliance [nm/mN]	0.3–0.4
Load noise floor [nN]	100	Specimen clamping [nm/mN]	~ 0.01
Maximum depth [μm]	15	Feedback control	Open loop
Displacement resolution [nm]	0.05–0.06	Drift correction	No

Table 2. Specifications of Nanotest 600 nanoindenter (values provided by the manufacturer and pretesting calibration). See also [Micromaterials 2002; Constantinides 2006].

$F_{\max}$ [mN]	31.45	$h_{\max}$ [nm]	2579
S [mN/nm]	0.0696	τ_L [sec]	3.12
M [GPa]	4.83	τ_H [sec]	29.99
H [GPa]	0.19	τ_U [sec]	4.14

Table 3. Indentation data for the Nanotest run.

indenter is assimilated to a cone of half-opening angle $\theta = 70.32°$. Table 2 provides more specifications on the nanoindenter device.

The load function is a prescribed trapezoidal force history:

$$F(t) = F_{\max} F(t), \qquad F(t) = \begin{cases} t/\tau_L & 0 \le t \le \tau_L, \\ 1 & \tau_L \le t \le \tau_L + \tau_H, \\ 1 - t/\tau_U & \tau_L + \tau_H \le t \le \tau_L + \tau_H + \tau_U. \end{cases} \tag{77}$$

The load was increased linearly up to $F_{\max}$, held constant during the creep phase and then decreased to zero linearly. In (77), τ_L, τ_H, and τ_U are, respectively, loading, holding, and unloading time which are given in Table 3. By monitoring force-indentation depth data (Figure 6), we get M and H from (1). Indentation parameters and moduli are summarized in Table 3.

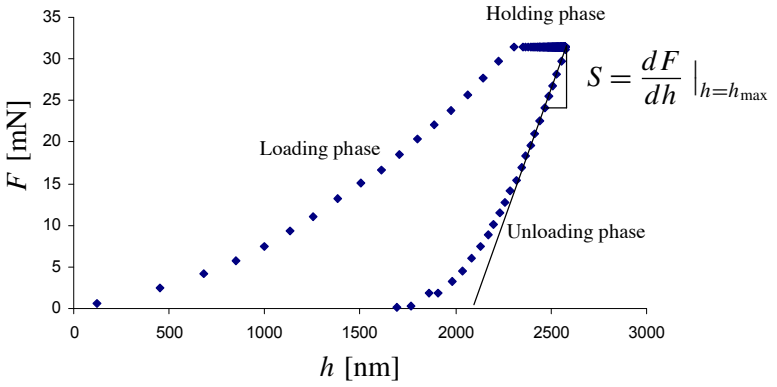

Figure 6. Load versus indentation depth for polystyrene.

Theoretical derivations throughout this paper are based on pure viscoelastic deformation. However, the monitored indentation depth is a mixture of elastic and plastic deformations, particular around the tip of the nanoindenter where there is a high stress concentration. Thus, in what follows, we first approximate the elastic indentation depth by removing the plastic indentation. Next, we fit the elastic experimental data to the theoretical creep compliance to identify the fractional model parameters.

5.1. ***Correcting for plasticity.*** Extensive works on plastic analysis of nanoindentation are available in the literature (see [Cheng and Cheng 2004], for example). Here we use the method proposed by Sakai in [Sakai 1999] and [Shimizu et al. 1999] to approximate the plastic deformations. In this method, the quadratic load-depth relations are experimentally observed through the relation

$$F = k_1 h^2. \tag{78}$$

Here k_1 is a parameter related to hardness H in $(1)_1$ and the true hardness H_T. For loading, k_1 reads

$$k_1 = \frac{gH}{\gamma^2}. \tag{79}$$

In this equation, γ is a geometrical factor which relates the total penetration depth h and the contact depth h_c through $h = \gamma h_c$ (we approximate $\gamma \approx 1$), and g is the geometrical factor of the indenter that relates to the contact area A_c by $g = A_c/h_c^2$. For a Berkovich indenter, $g = 24.5$. Sakai's analysis for elastoplastic indentation deformation is based on a Maxwell model in which $F = F_e = F_p$ and $h = h_e + h_p$ (indices e and p refer to elastic and plastic, respectively). This model consists of a perfectly elastic component with an elastic modulus M (as opposed to E) connected in series to a perfectly plastic component with true hardness H_T given by

$$H_T = \frac{k_1}{\left(\sqrt{g} - \sqrt{2\cot\theta}\sqrt{k_1/M}\right)^2}. \tag{80}$$

Plastic indentation can be computed from the quadratic relation between $F_p = F$ and h_p by

$$h_p(t) = \sqrt{\frac{F(t)}{gH_T}}. \tag{81}$$

Finally, $h_e(t)$, based on Sakai's procedure, is straightforward:

$$h_e(t) = h(t) - h_p(t). \tag{82}$$

During a creep test (constant load), $h_p(t)$ simplifies to a constant. By having indentation moduli in Table 3 and following (79) to (81), the plastic indentation depth during the holding phase is approximated to be $h_p = 1380\,\text{nm}$. In fact, it is implicitly assumed that there is no further plasticity during the creep test.

5.2. ***Viscoelastic fitting procedure.*** Now we consider fitting the approximated elastic data obtained experimentally to the viscoelastic model creep compliance. Direct fitting of the analytical solutions, (59) or (60), to the elastic experimental data in the time domain is a complicated task (because the analytical solutions require parametrically finding the roots of a rational function, Equation (58), with fractional exponents; see the Appendix). However, once the fractional and viscous parameters are known, Equations (59) and (60) are handy to use. In order to find the fractional and viscous parameters, we proceed in the following way, which leads to a curve-fitting in the Laplace domain:

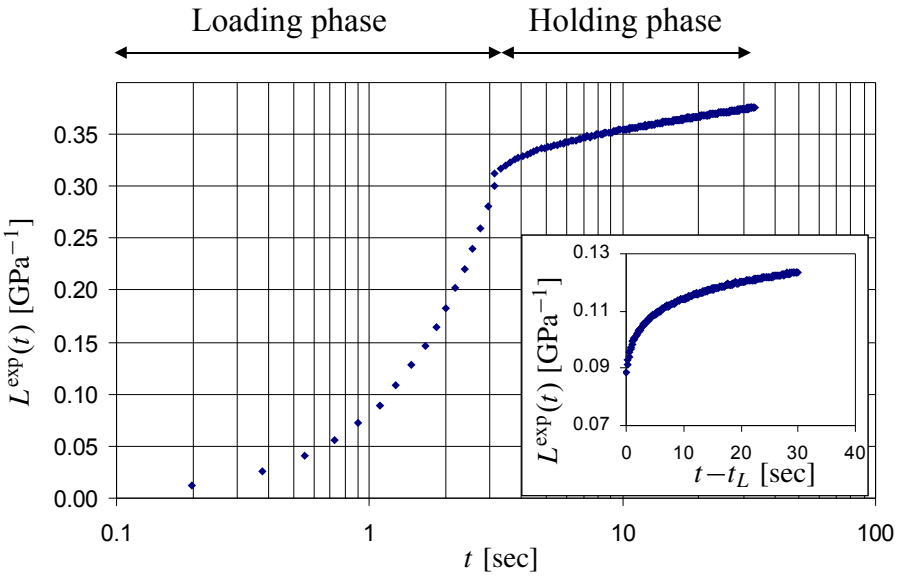

Figure 7. Time-dependent compliance $L(t)$ for polystyrene. The large window indicates $L^{\exp}(t)$ for the loading and holding phases ($0 < t < \tau_L + \tau_H$) where recorded experimental depth $h(t)$ is used; The small window shows $L_e^{\exp}(t)$ for the holding phase ($\tau_L < t < \tau_L + \tau_H$), where an elastic indentation depth $h_e(t)$ is used.

(i) From the recorded indentation depth $h(t)$, determine the experimental indentation creep compliance function $L^{\exp}$ for the equivalent cone representing the Berkovich indenter ($n = 1$, $B = \cot\theta$, see Table 1):

$$L^{\exp}(t) = \frac{\phi h^{1+1/n}(t)}{F_{\max}} = \frac{2\tan\theta}{\pi F_{\max}} h^2(t). \tag{83}$$

$L^{\exp}(t)$ is shown in the large window in Figure 7 and consists of the loading and the holding phases.

(ii) Focus on the creep response and consider the holding phase $t > \tau_L = 3.12\,\text{sec}$ where the load is constant. Determine elastic indentation depth $h_e(t)$ by using (79)–(82), and replace $h(t)$ by $h_e(t)$ in (83) to get the elastic compliance function $L_e^{\exp}(t)$. This is shown in the small window of Figure 7, and $L_e^{\exp}(t)$ reads

$$L_e^{\exp}(t) = \frac{\phi h^{1+1/n}(t)}{F_{\max}} = \frac{2\tan\theta}{\pi F_{\max}} h_e^2(t). \tag{84}$$

(iii) Transfer the time-dependent $L_e^{\exp}(t)$ to the Laplace domain. One can do this either numerically using a Finite Laplace Transform method, or by fitting a continuous function to $L_e^{\exp}(t)$ and then analytically transforming the fitted function to the Laplace space. We choose the latter procedure. By using a nonlinear optimization algorithm (for example, the `lsqnonlin` function in Matlab v7.4), it turns out that the best fitted function is a power function of the form

$$L_e^{\exp}(t) = at^b + c, \tag{85}$$

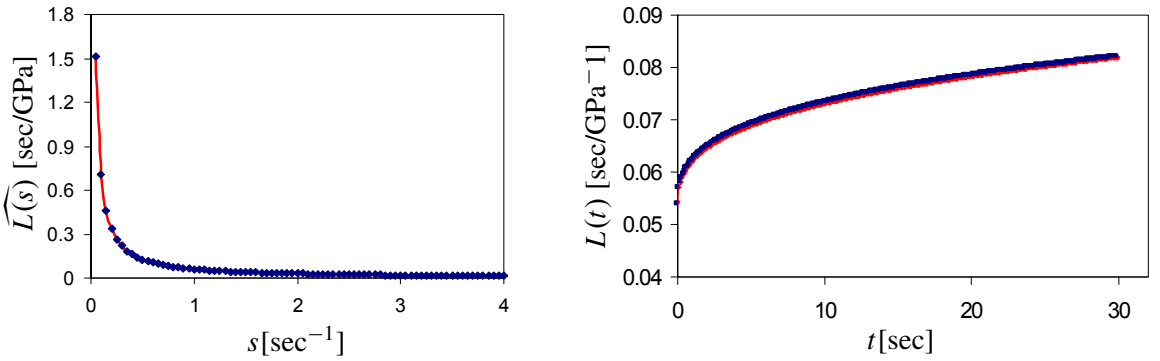

Figure 8. Left: curve-fitting in the Laplace domain for the compliance. Blue squares represent Laplace transform of experimental compliance $\widehat{L_e^{\exp}(s)}$ while the red line represents the Laplace of the theoretical model compliance $\widehat{L(s)}$. Right: validation of the curve-fitting in the time domain. Blue squares represent experimental compliance $L_e^{\exp}(t)$ and the red line represent theoretical model compliance $L(t)$ which perfectly coincides with $L_e^{\exp}(t)$.

where, for the test data in (84), $a = 0.0102$, $b = 0.318$, and $c = 0.052$. The parameter b is dimensionless, but $[a] = LM^{-1}T^{2-b}$ and $[c] = LM^{-1}T^2$. The Laplace transform of (85) is

$$\widehat{L_e^{\exp}(s)} = \frac{0.0102\Gamma(1+0.318)}{s^{1.318}} + \frac{0.052}{s}. \tag{86}$$

(iv) In Laplace space, fit the transformed elastic compliance response $\widehat{L_e^{\exp}(s)}$, given by (86), to the transformed model response $\widehat{L(s)}$ in (56), involving fractional exponents and parameters. In view of the considered models in Figure 4, this is equivalent to determining 10 independent unknown parameters in $\widehat{L(s)}$, namely α, Q_0, Q_1, Q_2, τ_v for the bulk and β, q_0, q_1, q_2, τ_d for the shear behavior. For the purpose of fitting in the complex plane, we refer to the Identity Theorem in complex analysis (for example, [Carrier et al. 1966; Marsden and Hoffman 1999]) and consider s as a real variable on the positive real axis. This fitting in the Laplace space does not require any a priori assumption of the particular model (double Maxwell, double Zener, etc.). Therefore, we minimize the quadratic error between the elastic compliance function, (86), and the model function (56) by

$$\min_{\substack{\alpha,\beta:\alpha<\beta,\\ Q_0,Q_1,Q_2,\tau_v\\ q_0,q_1,q_2,\tau_d}} \sum_{i=1}^{n+1} \left(\widehat{L_e^{\exp}(s_i)} - \frac{\widehat{D_F(s_i)}}{2s_i\,\widehat{D_h(s_i)}} \right)^2, \tag{87}$$

where the linear constraint $\alpha < \beta$ renders an account of the fact that the indentation test is more of a shear test, for which reason the effect of shear at the constitutive model is more influential. The result of this minimization yields the following values for the 10 parameters:

$$\begin{aligned} &\alpha = 0.257, \quad Q_0 = 3.37\,\text{GPa}, \quad Q_1 = 30.85\,\text{GPa}, \quad Q_2 = 58.01\,\text{GPa}, \quad \tau_v = 3.92\,\text{sec} \\ &\beta = 0.374, \quad q_0 = 0.84\,\text{GPa}, \quad q_1 = 13.99\,\text{GPa}, \quad q_2 = 59.46\,\text{GPa}, \quad \tau_d = 4.47\,\text{sec}. \end{aligned} \tag{88}$$

Since all parameters in (88) are nonzero, it is recognized that the tested material, polystyrene, follows best the double fractional Zener model with the sum of quadratic errors being 0.22×10^{-9}. By reducing the unknown parameters down to 8 for the double Maxwell models, this error becomes 3.1×10^{-9}. For validation, after identifying the model parameters of $\widehat{L(s)}$, the inverse Laplace transform of $L(s)$ must match with $L_e^{\exp}(t)$, (84), in the time domain. This is numerically confirmed in Figure 8 by using the Talbot algorithm [Abate and Valkó 2004]) for Laplace inversion.

Remark 1. Since s is, in general, a complex number, one may expect that both real and imaginary parts of s are required for the purpose of curve-fitting in the Laplace domain. But The Identity Theorem for single-valued analytic functions states that if two single-valued functions are analytic in a common region and coincide identically in a subset of that region (for instance, on a segment of a curve) then the two functions coincide identically throughout their common region of analyticity; see, for example, [Carrier et al. 1966; Marsden and Hoffman 1999]. A continuous function is analytic in a region of the complex plane if it is free of singularities in that region. Given that for any linear stable physical system, such as creep in indentation, $\widehat{L(s)}$ and $\widehat{L_e^{\exp}(s)}$ are free of singularities in the right-half of the complex plane where $\mathrm{Re}(s) > 0$ (see the Appendix), then if $\widehat{L(s)} = \widehat{L^{\exp}(s)}$ on the positive real axis of s (which is a subset of the complex plane in which $\widehat{L(s)}$ and $\widehat{L_e^{\exp}(s)}$ are analytic), then directly from the Identity Theorem, $\widehat{L(s)} = \widehat{L_e^{\exp}(s)}$ throughout all regions of their analyticity in the complex plane. Hence, for fitting $\widehat{L(s)}$ and $\widehat{L_e^{\exp}(s)}$ on the complex plane, as long as these functions coincide in a region where s lies on the positive real axis, there is no need for the imaginary parts of s to be taken into account. Here we used a relatively large interval up to $s = 1000\,\mathrm{sec}^{-1}$ (since the exponent of e^{st} is dimensionless, the dimension of s is 1/time which indicates that large s refers to small times and small s to large times). Increasing this interval is practically insignificant because $\widehat{L_e^{\exp}(s)}$ approaches zero at around $s = 4\,\mathrm{sec}^{-1}$ (Figure 8).

Remark 2. The optimization problem (87) defined in the Laplace domain involves a ten-dimensional shallow hypersurface for the ten unknown parameters $(\alpha, Q_0, Q_1, Q_2, \tau_v, \beta, q_0, q_1, q_2, \tau_d)$, in which there are many local minima. To approach the global minimum, we use ten nested loops over initial parameter guesses, each loop covering the given range of that parameter (we consider $0 < \alpha, \beta < 1$ and $0 < \tau_v, \tau_d < 10\,\mathrm{sec}$, $0 < Q_0, Q_1, Q_2, q_0, q_1, q_2 < 70\,\mathrm{GPa}$). We then regularly discretize the range of each parameter and repeat the optimization as many times as different combinations of initial parameter guesses exist through the ten nested loops.

Remark 3. The optimization algorithm starts from different points within the hypersurface and each time finds a closest local minimum by calling the 'lsqnonlin' subroutine in Matlab v7.4, which uses a subspace trust region method for each set of initial parameter guesses. This subroutine is based on the interior-reflective Newton method [Coleman and Li 1994; 1996], and is set to a maximum of 20,000 iterations and function evaluations. Each iteration in this subroutine involves the approximate solution of the large linear system using the method of preconditioned conjugate gradients (PCG). Over all initial parameter guesses, the criterion for the best fit (or the global minimum among these local minima) will be the one that has the least quadratic error. For a double Zener model, the run time for finding the global minimum was 2 days, and the mean and standard deviation of the minima are 1.8×10^{-5} and 2.9×10^{-4}, respectively.

Given that the quadratic error function for the global minimum is orders of magnitude less than the mean of the minima, the objective function must be highly sensitive to the model parameters. To clarify this dependence we perform a sensitivity analysis.

5.3. ***Sensitivity analysis of the model parameters.*** Once the model parameters are identified, one can perform a sensitivity analysis to determine the quality of the employed models and the parameters that contribute most to the output variability, which in this case is the objective function (88). Sensitivity analysis also enables us to study the optimal– or instability– regions within the space of each parameter for which the objective function is guaranteed not to jump from the global minimum to the next lowest local minimum. Let's use the symbol Θ to indicate the objective function (88). We numerically disturb a model parameter, say α, from its optimum value while keeping all the other model parameters unchanged. Next, by monitoring the change in Θ to a defined tolerance $\Delta\Theta$, we can measure the sensitivity of Θ with respect to each model parameter. Then, one can simply repeat this procedure for each model parameter and find a tolerance in which Θ is assured not to exceed the allowable drift. Here, for a double Zener model, we set $\Delta\Theta = (0.59 - 0.22) \times 10^{-9} = 0.37 \times 10^{-9}$, which is the difference between the global minimum Θ and its next lowest local minimum. For this case, we obtain

$$\begin{aligned} &\Delta\alpha = \pm 0.0001, \quad \Delta Q_0 = \pm 0.7\,\text{MPa}, \ \Delta Q_1 = \pm 2.1\,\text{MPa}, \ \Delta Q_2 = \pm 5.6\,\text{MPa}, \ \Delta\tau_v = \pm 0.0015\,\text{sec}, \\ &\Delta\beta = \pm 0.00004, \quad \Delta q_0 = \pm 0.2\,\text{MPa}, \quad \Delta q_1 = \pm 0.3\,\text{MPa}, \quad \Delta q_2 = \pm 3.6\,\text{MPa}, \ \Delta\tau_d = \pm 0.0007\,\text{sec}. \end{aligned} \tag{89}$$

In view of (89), the following observations are in order:

1. All parameters on the second line of (89) which are related to the deviatoric Zener model, are less than their counterpart on the first line, which are related to the volumetric Zener model. This suggests that the creep phenomenon during indentation is more sensitive to the deviatoric (shear) behavior. In other words, the time-dependent response of the shear behavior is more pronounced than that of the bulk behavior.
2. For each of the deviatoric and volumetric Zener models, the fractional parameters α and β, with the least tolerance, are the most sensitive parameters in the quadratic error function, or, alternatively, the most dominant parameters in the time-dependent response function.
3. Among all the parameters of the two models, the β parameter in the deviatoric model is the most sensitive factor in the error function (equivalently, the most dominant factor for the time-dependent response function), followed by α, which is the second most dominant (second least sensitive) parameter in the response function.

The results of the sensitivity analysis are in agreement with the observation that the effect of β (or shear) dominates over the effect of α. In fact, Θ is a nonlinear rational function of the independent variable s, the model parameters $(\alpha, Q_0, Q_1, Q_2, \tau_v)$ for bulk and $(\beta, q_0, q_1, q_2, \tau_d)$ for shear behavior. Among these parameters, the fractional parameters α, β have significant influence in determining Θ. This is because α, β appear as the exponents of s in Θ. For instance, in the case of shear behavior, in view of $(28)_1$ and (33), it is readily seen that the other four viscous model parameters appear only as coefficients of s,and thus their variations are not as critical as β. Then, between α and β, β, with greater exponent, is clearly the dominant parameter.

6. Conclusions

The fractional viscoelastic model offers new possibilities for the characterization of materials whose time-dependent response may be poorly captured by classical integer-type viscoelastic models. The analysis and method developed in this paper aims at determining the fractional properties from indentation analysis. The following conclusions can be drawn:

(i) The derived constitutive differential equations governing the indentation response show that the differential order of the constitutive differential equations of the indentation response is higher than the one governing the material level. This difference in differential order between the material scale and indentation scale holds for both fractional and integer-type viscoelastic models, the latter being recognized as a subset of the more general fractional modeling framework. The found difference is more pronounced for the viscoelastic shear response than for the viscoelastic bulk response. This is explicitly shown with higher order derivatives in β than in α for fractional viscoelastic materials. This observation is in agreement with the sensitivity analysis performed on the error function, and it translates into the well-known fact that an indentation test is rather a shear test than a hydrostatic test.

(ii) The general constitutive differential equations are readily employed to derive indentation creep and relaxation functions, which, analogously to uniaxial creep compliance and relaxation functions, can be used in fractional indentation analysis for any monotonically increasing force- or depth-load histories applied in indentation testing. On this basis, explicit solutions for specific fractional creep models can be derived, as illustrated for the double Zener, double Maxwell, and deviatoric Maxwell and Zener models.

(iii) In order to translate time-dependent indentation data into fractional material model properties, we suggest fitting the experimental response to the model response in the Laplace domain. This reduces the mathematical complexity of obtaining properties from indentation data without compromising the accuracy of the fit in the time domain. Our optimization method has two important features: the optimum model parameters do not depend on the initial parameter guesses; and in our curve-fitting on the complex plane, all functions are treated as real functions by making use of the Identity Theorem.

Appendix

The fractional expression $\widehat{D(s)}$ can be converted into a polynomial of integer order by

$$\widehat{D(s)} = \sum_j b_j s^{j/m} = \sum_j b_j u^j = X(u), \tag{90}$$

where $u^j = s^{j/m}$, and $m > 0$ is the smallest common denominator of the fractional parameters α and β. Some of the coefficients b_j are clearly zero, while any non-zero b_j corresponds to the coefficient of s in $\widehat{D(s)}$ whose exponent becomes equal to j/m. The inverse transform of a function, $\widehat{f(s)}$, exists and is real, continuous, and causal when (i) $\widehat{f(s)}$ is analytic for $\mathrm{Re}(s) > 0$, (ii) $\widehat{f(s)}$ is real for s real and positive, (iii) $\widehat{f(s)}$ is of order $s^{-\gamma}$, where $\gamma > 1$, for $|s|$ large in the right half s plane [Churchill 1958]. One can simply show that $\widehat{L(s)}$ in (56) satisfies all three conditions. By definition, the inverse Laplace

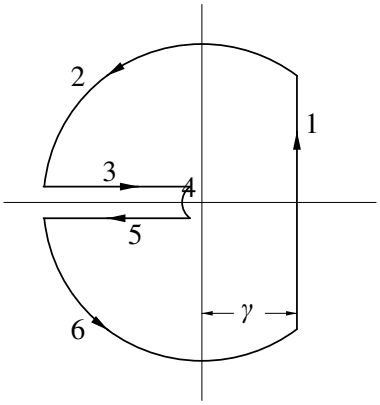

Figure 9. Integration contour on the complex s-plane for the calculation of (91).

transform of (56) is then

$$L(t) = \frac{1}{2\pi i} \int_{\gamma - i\infty}^{\gamma + i\infty} e^{st} \frac{\widehat{D_F(s)}}{2s\widehat{D_h(s)}}\, ds. \tag{91}$$

One can evaluate this line integral by extending it into a closed contour integration, as in Figure 9. Recall that the residue theorem states that the integral along any closed contour, divided by $2\pi i$, is equal to the sum of the residues of poles of the integrand within that contour. The contour in Figure 9, is divided into six segments with arrows which indicate the direction of integration. (Segments 3, 4, 5 are needed since the branch cut of $s^{1/m}$ lies along the negative real axis.) We thus can write

$$\frac{1}{2\pi i} \int_{C_1} e^{st} \frac{\widehat{D_F(s)}}{2s\widehat{D_h(s)}} ds + \frac{1}{2\pi i} \sum_{k=2}^{6} \int_{C_k} e^{st} \frac{\widehat{D_F(s)}}{2s\widehat{D_h(s)}} ds = \sum_j b_j, \tag{92}$$

where b_j are the residues. Equation (91) is the first term in (92) when its limits are extended to infinity in the negative and positive imaginary directions of the s plane. The radii of the segments 2 and 6 are increased infinitely to ensure the continuity of the closed contour. Similarly, segments 3 and 5 are stretched to infinity on the negative real axis. When the radius approaches infinity, it can be shown that the integrals along the contours 2 and 6 are zero. By using the following lemma [MacRobert 1962] one can obtain the contour integral along the segment 4,

Lemma. *If* $\lim(s-a)f(s) = k$ *as* $s \to a$, *where* k *is a constant, then* $\lim \int f(s)ds = i(\theta_2 - \theta_1)k$, *the integral being taken for* $s \to a$ *and* $r \to 0$ *around an arc from* θ_1 *to* θ_2 *of the circle* $|s-a| = r$.

It follows that since $(\theta_2 - \theta_1) = 0$,

$$\int_4 e^{st} \frac{\widehat{D_F(s)}}{2s\widehat{D_h(s)}} ds = 0. \tag{93}$$

One can also show that

$$\int_3 e^{st} \frac{\widehat{D_F(s)}}{2s\widehat{D_h(s)}} ds + \int_5 e^{st} \frac{\widehat{D_F(s)}}{2s\widehat{D_h(s)}} ds = -2i \operatorname{Im} \int_0^{\infty} e^{-rt} \frac{\widehat{D_F(re^{-i\pi})}}{2s\widehat{D_h(re^{-i\pi})}}\, dr. \tag{94}$$

Finally, using the conventional technique, the residues are calculated as

$$b_j = \lim_{s\to\lambda_j^m}(s-\lambda_j^m)\frac{\widehat{D_F(s)}}{2s\widehat{D_h(s)}}e^{st}. \tag{95}$$

Here, λ_j refers to the j-th root of the integer polynomial $X(u)$. In view of equations (90) and (56), the roots of $X(u)$ correspond to the poles of $L(t)$. Lastly, by substituting (93), (94), and (95) into (92), one can find the general solution in the time domain. For specific solutions, we need to consider different models. For a double Zener models, since all the c and l coefficients in (42) are nonzero, $s=0$ in (56) is a simple pole, and because its exponent is one and an integer number, this pole is on the s-plane. Thus, its residue via (95) is simply the first term in (59). Other poles of (56) λ_i (those that make $\widehat{D_h(s)}=0$) were found in the $s^{1/m}$ plane. Since the Laplace transform is performed in the s-plane, the poles λ_i should be transformed into λ_i^m to be on the s-plane. However, that transformation maps some of the original poles onto Riemann surfaces out of the closed contour of integration in the $s-$plane. Thus, according to the residue theorem, the residues of such poles do not contribute to the solution. Hence, the summation over the index j in (59) (and through all equations in this paper) pertains only to those poles that remain in the closed contour's plane after the transformation. This indicates that, for a linear physical system, λ_i^m must have a negative real part in order for the system to be stable.

For double Maxwell models, $c_0=l_0=l_1=l_2=0$, and (56) simplifies to

$$\widehat{L(s)}=\frac{\widehat{D_F(s)}}{2s\widehat{D_h(s)}}=\frac{c_1s^\alpha+c_2s^\beta+c_3s^{\alpha+\beta}+c_4s^{\alpha+2\beta}+c_5s^{2\beta}}{2s(l_3s^{\alpha+\beta}+l_4s^{\alpha+2\beta}+l_5s^{2\beta})}. \tag{96}$$

In the case of $\alpha\le\beta$, after cancelling out s^α, (96) yields

$$\widehat{L(s)}=\frac{c_1+c_2s^{\beta-\alpha}+c_3s^\beta+c_4s^{2\beta}+c_5s^{2\beta-\alpha}}{2s^{1+\beta}(l_3+l_4s^\beta+l_5s^{\beta-\alpha})}. \tag{97}$$

Clearly, $s=0$ in (97) is not a simple pole, rather, it is a pole of fractional order $1+\beta$. Consider this fractional number to be k/m, where k and m are two integer numbers. By using the following transformation:

$$s^{1+\beta}=(s^{1/m})^k=u^k, \tag{98}$$

one can convert (97) into quotient of two polynomials as

$$\widehat{L(u)}=\frac{c_1+c_2u^{m(\beta-\alpha)}+c_3u^{m\beta}+c_4u^{2m\beta}+c_5u^{m(2\beta-\alpha)}}{2u^k(l_3+l_4u^{m\beta}+l_5u^{m(\beta-\alpha)})}. \tag{99}$$

Now, $u=0$ in (99) is a multiple pole of order k. In order to find its residue, we use the fact that the residue of a function $f(s)=Q(s)/(s-a)^{n+1}$ at a multiple pole a of order $n+1$ is given by

$$F(s,t)=\frac{1}{n!}\frac{\partial^n}{\partial^n s}[Q(s)e^{st}]_{s=a}.$$

(see [Churchill 1958], for example). Applying this to (99) leads to $(61)_1$. Similarly, in the case of $\alpha>\beta$, after cancelling out s^β, one can find $(61)_2$. The residue theorem in conjunction with fractional-order derivatives has been used in [Bagley and Torvik 1983] and [Ostoja-Starzewski and Shahsavari 2008] in a slightly different way.

References

[Abate and Valkó 2004] J. Abate and P. P. Valkó, "Multi-precision Laplace transform inversion", *Int. J. Numer. Methods Eng.* **60** (2004), 979–993.

[Arkhincheev 1993] V. E. Arkhincheev, "Anomalous diffusion in inhomogeneous media: some exact results", *Model. Meas. Control A* **26**:2 (1993), 11–29.

[Bagley and Torvik 1983] R. L. Bagley and P. J. Torvik, "A theoretical basis for the application of fractional calculus to viscoelasticity", *J. Rheol.* **27**:3 (1983), 201–210.

[Baker et al. 1996] W. P. Baker, L. B. Eldred, and A. Palazotto, "Viscoelastic material response with a fractional-derivative constitutive model", *AIAA J.* **34**:3 (1996), 596–600.

[Bland 1960] D. R. Bland, *The theory of linear viscoelasticity*, International Series of Monographs on Pure and Applied Mathematics **10**, Pergamon, New York, 1960.

[Borodich and Galanov 2008] F. M. Borodich and B. A. Galanov, "Non-direct estimations of adhesive and elastic properties of materials by depth-sensing indentation", *Proc. R. Soc. Lond. A* **464**:2098 (2008), 2759–2776.

[Borodich and Keer 2004] F. M. Borodich and L. M. Keer, "Contact problems and depth-sensing nanoindentation for frictionless and frictional boundary conditions", *Int. J. Solids Struct.* **41**:9–10 (2004), 2479–2499.

[Boussinesq 1885] J. Boussinesq, *Applications des potentiels à l'étude de l'équilibre et du mouvement des solides élastiques*, Gauthier-Villars, Paris, 1885.

[Brinell 1901] J. A. Brinell, "Mémoire sur les épreuves à bille en acier", pp. 83–94 in *Communications presentés devant le Congrés International des Méthodes d'Essai des Matériaux de Construction* (Paris, 1900), vol. 2, edited by P. Debray and L. Baclé, Dunod, Paris, 1901.

[Bulychev 1999] S. I. Bulychev, "Relation between the reduced and unreduced hardness in nanomicroindentation tests", *Tech. Phys.* **44**:7 (1999), 775–781.

[Caputo 1967] M. Caputo, "Linear models of dissipation whose Q is almost frequency independent, Part II", *Geophys. J. Int.* **13**:5 (1967), 529–539.

[Caputo 1969] M. Caputo, *Elasticità e dissipazione*, Zanichelli, Bologna, 1969.

[Cariou et al. 2008] S. Cariou, F.-J. Ulm, and L. Dormieux, "Hardness-packing density scaling relations for cohesive-frictional porous materials", *J. Mech. Phys. Solids* **56**:3 (2008), 924–952.

[Carrier et al. 1966] G. F. Carrier, M. Krook, and C. E. Pearson, *Functions of a complex variable: theory and technique*, McGraw-Hill, New York, 1966.

[Cheng and Cheng 2004] Y.-T. Cheng and C.-M. Cheng, "Scaling, dimensional analysis, and indentation measurements", *Mater. Sci. Eng. R* **44**:4–5 (2004), 91–149.

[Cheng et al. 2000] L. Cheng, H. Xia, W. Yu, L. E. Scriven, and W. W. Gerberich, "Flat-punch indentation of viscoelastic materials", *J. Polym. Sci. B Polym. Phys.* **38**:1 (2000), 10–22.

[Cheng et al. 2005] L. Cheng, X. Xia, L. E. Scriven, and W. W. Gerberich, "Spherical-tip indentation of viscoelastic material", *Mech. Mater.* **37**:1 (2005), 213–226.

[Christensen 1971] R. M. Christensen, *Theory of viscoelasticity: an introduction*, Academic Press, New York, 1971.

[Churchill 1958] R. V. Churchill, *Operational mathematics*, 2nd ed., McGraw-Hill, New York, 1958.

[Coleman and Li 1994] T. F. Coleman and Y. Li, "On the convergence of interior-reflective Newton methods for nonlinear minimization subject to bounds", *Math. Program.* **67**:2, Ser. A (1994), 189–224.

[Coleman and Li 1996] T. F. Coleman and Y. Li, "An interior trust region approach for nonlinear minimization subject to bounds", *SIAM J. Optim.* **6**:2 (1996), 418–445.

[Constantinides 2006] G. Constantinides, *Invariant mechanical properties of Calcium-Silicate-Hydrates (C-S-H) in cement-based materials: instrumented nanoindentation and micromechanical modeling*, Ph.D. thesis, Department of Civil and Environmental Engineering, Massachusetts Institute of Technology, 2006.

[Doerner and Nix 1986] M. F. Doerner and W. D. Nix, "A method for interpreting the data from depth-sensing indentation instruments", *J. Mater. Res.* **1**:4 (1986), 601–609.

[Engheta 1996] N. Engheta, "On fractional calculus and fractional multipoles in electromagnetism", *IEEE Trans. Antenn. Propag.* **44**:4 (1996), 554–566.

[Flügge 1967] W. Flügge, *Viscoelasticity*, Blaisdell, Waltham, MA, 1967.

[Galanov 1982] B. A. Galanov, "An approximate method for the solution of some two-body contact problems with creep in the case of an unknown contact area", *Sov. Appl. Mech.* **18**:8 (1982), 711–718.

[Galin 1961] L. A. Galin, *Contact problems in the theory of elasticity*, edited by I. N. Sneddon, North Carolina State College, Raleigh, NC, 1961.

[Ganneau et al. 2006] F. P. Ganneau, G. Constantinides, and F.-J. Ulm, "Dual-indentation technique for the assessment of strength properties of cohesive-frictional materials", *Int. J. Solids Struct.* **43**:6 (2006), 1727–1745.

[Gao and Ogden 2003] D. Y. Gao and R. W. Ogden (editors), *Advances in mechanics and mathematics, Volume II*, Advances in Mechanics and Mathematics **4**, Kluwer Academic, Boston, 2003.

[Glöckle and Nonnenmacher 1991] W. G. Glöckle and T. F. Nonnenmacher, "Fractional integral operators and Fox functions in the theory of viscoelasticity", *Macromolecules* **24**:24 (1991), 6426–6434.

[Hertz 1882] H. Hertz, "Über die Berührung fester elastischer Körper", *J. Reine Angew. Math.* **92** (1882), 156–171. Translated in *Miscellaneous papers by H. Hertz*, Jones and Schott (Eds.), Macmillan, London, 1896.

[Kilbas et al. 2006] A. A. Kilbas, H. M. Srivastava, and J. J. Trujillo, *Theory and applications of fractional differential equations*, North-Holland Mathematics Studies **204**, Elsevier, Amsterdam, 2006.

[Lee 1955] E. H. Lee, "Stress analysis in visco-elastic bodies", *Quart. Appl. Math.* **13** (1955), 183–190.

[Lee and Radok 1960] E. H. Lee and J. R. M. Radok, "The contact problem for viscoelastic bodies", *J. Appl. Mech.* (*ASME*) **27** (1960), 438–444.

[Love 1939] A. E. H. Love, "Boussinesq's problem for a rigid cone", *Quart. J. Math. Oxford Ser.* (*2*) **10**:1 (1939), 161–175.

[MacRobert 1962] T. M. MacRobert, *Functions of a complex variable*, 5th ed., Macmillan, London, 1962.

[Marsden and Hoffman 1999] J. E. Marsden and M. J. Hoffman, *Basic complex analysis*, 3rd ed., W. H. Freeman, New York, 1999.

[Micromaterials 2002] *Micromaterials nanotest user manual*, Micromaterials, Wrexhham, 2002.

[Oliver and Pharr 1992] W. C. Oliver and G. M. Pharr, "An improved technique for determining hardness and elastic modulus using load and displacement sensing indentation experiments", *J. Mater. Res.* **7**:6 (1992), 1564–1583.

[Ostoja-Starzewski and Shahsavari 2008] M. Ostoja-Starzewski and H. Shahsavari, "Response of a helix made of a fractional viscoelastic material", *J. Appl. Mech.* (*ASME*) **75**:1 (2008), 011012.

[Oyen 2005] M. L. Oyen, "Spherical indentation creep following ramp loading", *J. Mater. Res.* **20**:8 (2005), 2094–2100.

[Oyen 2006] M. L. Oyen, "Analytical techniques for indentation of viscoelastic materials", *Philos. Mag.* **86**:33–35 (2006), 5625–5641.

[Podlubny 1999] I. Podlubny, *Fractional differential equations*, Mathematics in Science and Engineering **198**, Academic Press, San Diego, CA, 1999.

[Rabotnov 1980] J. N. Rabotnov, *Elements of hereditary solid mechanics*, Mir, Moscow, 1980.

[Radok 1957] J. R. M. Radok, "Visco-elastic stress analysis", *Quart. Appl. Math.* **15** (1957), 198–202.

[Ross 1977] B. Ross, "Fractional calculus", *Math. Mag.* **50**:3 (1977), 115–122. An historical apologia for the development of a calculus using differentiation and antidifferentiation of non-integral orders.

[Rossikhin and Shitikova 2004] Y. A. Rossikhin and M. V. Shitikova, "Analysis of the viscoelastic rod dynamics via models involving fractional derivatives or operators of two different orders", *Shock Vib. Digest* **36**:1 (2004), 3–26.

[Sakai 1999] M. Sakai, "The Meyer hardness: a measure for plasticity?", *J. Mater. Res.* **14**:9 (1999), 3630–3639.

[Schiessel and Blumen 1993] H. Schiessel and A. Blumen, "Hierarchical analogues to fractional relaxation equations", *J. Phys. A Math. Gen.* **26**:19 (1993), 5057–5069.

[Schiessel et al. 1995] H. Schiessel, R. Metzler, A. Blumen, and T. F. Nonnenmacher, "Generalized viscoelastic models: their fractional equations with solutions", *J. Phys. A Math. Gen.* **28**:23 (1995), 6567–6584.

[Shahsavari and Ostoja-Starzewski 2005] H. Shahsavari and M. Ostoja-Starzewski, "On elastic and viscoelastic helices", *Philos. Mag.* **85**:33–35 (2005), 4213–4230.

[Shimizu et al. 1999] S. Shimizu, T. Yanagimoto, and M. Sakai, "Pyramidal indentation-depth curve of viscoelastic materials", *J. Mater. Res.* **14**:10 (1999), 4075–4086.

[Sneddon 1965] I. N. Sneddon, "The relation between load and penetration in the axisymmetric Boussinesq problem for a punch of arbitrary profile", *Int. J. Eng. Sci.* **3**:1 (1965), 47–57.

[Tabor 1951] D. Tabor, *Hardness of metals*, Clarendon, Oxford, 1951.

[Tschoegl et al. 2002] N. W. Tschoegl, W. G. Knauss, and I. Emri, "Poisson's ratio in linear viscoelasticity: a critical review", *Mech. Time-Depend. Mat.* **6**:1 (2002), 3–51.

[Vandamme and Ulm 2006] M. Vandamme and F.-J. Ulm, "Viscoelastic solutions for conical indentation", *Int. J. Solids Struct.* **43**:10 (2006), 3142–3165.

[Vandamme and Ulm 2007] M. Vandamme and F.-J. Ulm, "Indenter-shape independent viscoelastic solutions for indentation creep and relaxation testing", *C. R. Mécanique* (2007). Submitted.

Received 12 Oct 2008. Revised 22 Dec 2008. Accepted 4 Feb 2009.

ROUZBEH SHAHSAVARI: shahs@mit.edu
Department of Civil and Environmental Engineering, Massachusetts Institute of Technology, 77 Massachusetts Avenue, Cambridge, MA 02139-4307, United States

FRANZ-JOSEF ULM: ulm@mit.edu
Department of Civil and Environmental Engineering, Massachusetts Institute of Technology, 77 Massachusetts Avenue, Cambridge, MA 02139-4307, United States